

## AUTHOR QUERIES

### AUTHOR PLEASE ANSWER ALL QUERIES

**PLEASE NOTE:** We cannot accept new source files as corrections for your article. If possible, please annotate the PDF proof we have sent you with your corrections and upload it via the Author Gateway. Alternatively, you may send us your corrections in list format. You may also upload revised graphics via the Author Gateway.

AQ:1 = Please supply index terms/keywords for your article. To download the IEEE Taxonomy, go to [http://www.ieee.org/documents/taxonomy\\_v101.pdf](http://www.ieee.org/documents/taxonomy_v101.pdf).

AQ:2 = Please confirm or add details for any funding or financial support for the research of this article.

AQ:3 = Please provide the issue no. or month for Ref. [1], [5], [13], [15], and [26].

AQ:4 = Please provide the journal title for Ref. [3].

AQ:5 = Note that Refs. [14] and [19] were identical in your originally submitted manuscript. Hence, we have deleted Ref. [19] and renumbered the subsequent references. This will also be reflected in the citations present in the body text. Please confirm.

AQ:6 = Please provide the year of completion when the author Eli Leinov received the B.Sc., M.Sc., and Ph.D. degrees.

AQ:7 = Please provide the city name for Ben-Gurion University.

AQ:8 = Please provide the year of completion when the author Alejandro Jeketo received the M.Eng. and Eng.D. degrees.

AQ:9 = Please provide the year of completion when the author “Michael J. S. Lowe” received the B.Sc., M.Sc., and Ph.D. degrees.

# A Guided Wave Inspection Technique for Wedge Features

Joseph Corcoran<sup>1</sup>, Eli Leinov<sup>2</sup>, Alejandro Jeketo, and Michael J. S. Lowe



Fig. 1. Photograph of engine drum with inset CAD render of a feature composed of four wedge-like seal fins, the upper two are 2 mm in height and the lower two are 4 mm.

(see Fig. 1) as an example, but the outcomes are widely applicable. Aero engines comprise a number of stages between which temperature and pressure are changed to ultimately generate thrust. The thermodynamic performance of the engine is improved by seal fins—wedge shaped structures a few millimeters in height that run circumferentially between stages and reduce interstage leakage. The inspection requirement in this example is to detect 0.75-mm radial tip defects; this is a crack that is the full width of the wedge, measured from the tip of the wedge to the base and orientated normal to the axial direction of the wedge. The presence of an abrasive coating and restricted access means that scanning along the length of the seal-fin feature is not possible and so a method for screening along the length of the feature from a single location is sought.

Antisymmetric flexural edge modes (“edge modes”) can propagate in wedge features, as shown in Fig. 2. Multiple orders of edge modes may exist in a wedge feature, with subsequent orders having increasing numbers of nodes, as shown in Fig. 2(b) and (c); throughout this article, the first-order wedge mode will be of primary interest, but higher order modes will be discussed where relevant. Wedge modes were discovered by Lagasse [1] and have since been studied

**Abstract**—Numerous engineering components feature prismatic wedge-like structures that require nondestructive evaluation (NDE) in order to ensure functionality or safety. This article focuses on the inspection of the wedge-like seal fins of a jet engine drum, though the capabilities presented will be generic. It is proposed that antisymmetric flexural edge modes, feature-guided waves localized to the wedge tips, may be used for defect detection. Although analytical solutions exist that characterize the ultrasonic behavior of ideal wedges, in practice, real wedges will be irregular (containing, for example, truncated tips that are built onto an associated structure or have nonstraight edges), and therefore, generic methodologies are required to characterize wave behavior in nonideal wedges. This article uses a semianalytical finite-element (SAFE) methodology to characterize the guided waves in wedge-like features with irregular cross sections to assess their suitability for NDE inspection and compare them with edge modes in ideal wedges. The science and methodologies required in this article are necessary to select an appropriate operating frequency for the particular application at hand. In addition, this article addresses the practical challenge of excitation and detection of flexural edge modes by presenting a piezoelectric-based dry-coupled transducer system suitable for pulse-echo operation. This article, therefore, presents the scientific basis required for industrial exploitation, together with the practical tools that facilitate use. The study concludes with the experimental demonstration of the edge wave-based inspection of a seal fin, achieving a signal-to-noise ratio of 28 dB from a 0.75-mm radial tip defect.

**Index Terms**—XXXXX.

## I. INTRODUCTION

WEDGE-LIKE features are built on a range of engineering components forming, for example, blades, cutting disks, and seals. To maintain the safety and proper function of these features, it may be necessary to undertake nondestructive evaluation (NDE) to screen for defects or damage, especially at the wedge tips. In this article, we focus on the application of the seal fins that separate pressure stages of a jet engine

Manuscript received October 2, 2019; accepted December 5, 2019. (Corresponding author: Joseph Corcoran.)

Joseph Corcoran and Michael J. S. Lowe are with the Department of Mechanical Engineering, Imperial College London, London SW7 2AZ, U.K. (e-mail: joseph.corcoran@imperial.ac.uk).

Eli Leinov is with the Department of Mechanical Engineering, Imperial College London, London SW7 2AZ, U.K., and also with Guided Ultrasonics Ltd., Brentford TW8 8HQ, U.K.

Alejandro Jeketo is with Rolls-Royce plc, Derby DE24 8BJ, U.K. Digital Object Identifier 10.1109/TUFFC.2019.2960108

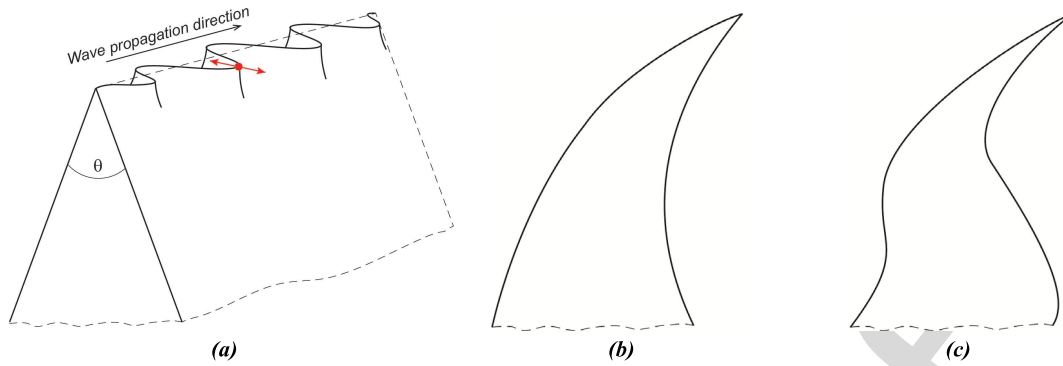


Fig. 2. (a) Illustration of the antisymmetric flexural edge mode, following [4]. Included in red is an illustration of the transducer motion required for excitation and detection of the flexural edge mode. Typically, it is assumed that the transducer footprint should be less than one-fifth of the wavelength. (b) Illustration of the first-order flexural edge mode. (c) Illustration of the second-order flexural edge mode.

in the literature theoretically and experimentally for a few decades [2]–[4]. The desirable characteristics of such modes for NDE are noted in the literature [4], [5], and the waves are guided along the length of the feature with the energy localized to the apex of the wedge; this makes the modes well suited for screening wedge tips in long features. Despite the numerous positive attributes of the edge wave, to date, there has been little reported use in industrial applications. This study aims to address some of the issues limiting uptake, namely, determining dispersion characteristics and localization of ultrasonic energy in irregular wedge-like features, and developing a means of excitation and detection. While recent literature on wedge modes' propagation has been mainly focused on the damping characteristics of wedges as a means to reduce structural vibration [6], [7], their application in NDT has been limited mainly due to the complexity of their defect-scattering phenomena [8], [9].

For effective implementation of an inspection procedure, the dispersion characteristics will need to be evaluated. In an ideal wedge cross section (infinite length, nontruncated, symmetric, and straight-edged), the edge modes are nondispersive with the geometry described by a single nondimensional parameter, the wedge angle  $\theta$ , as shown in Fig. 2(a) [4]. However, in all real components, the wedge features will be nonideal as they will be of finite length and may be built into a larger structure, and their tip will be truncated to some extent. In nonideal wedge features, the finite geometry makes the edge mode dispersive at the low frequencies that are desirable for practical application; though analytical models describing the influence of some of the irregular wedge-like structures have been proposed [4], [10], it may be difficult to apply them broadly to practical applications. Semianalytical finite-element (SAFE) analysis will be used throughout this study to characterize the ultrasonic behavior in the wedge-like structures. SAFE is an established method for evaluating wave behavior in waveguides of arbitrarily shaped cross section (for example, railway lines [11], [12], beams [12], [13], and stiffeners [14]–[16]) and in feature-guided waves (such as bends [17], [18] and welds [14], [19]). This study extends the current capabilities by specifically addressing waves in irregular wedge-like features and at low frequencies where dispersion may be significant. SAFE will be used to assess the dispersion characteristics, the leakage of the waves into the

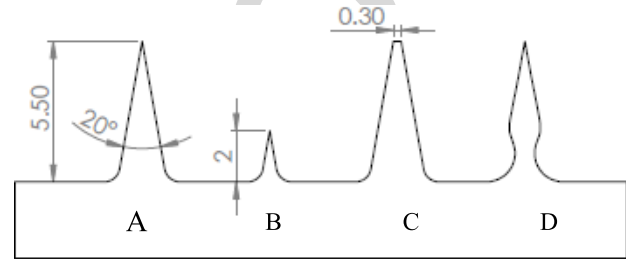


Fig. 3. Illustration of the hypothetical component with four different wedge-like features. A: Most ideal of the wedges. B: Shortened length. C: Truncated apex. D: Nonstraight sided. All dimensions in millimeters and degrees.

TABLE I  
ASSUMED MATERIAL PROPERTIES OF IN718  
USED THROUGHOUT THIS STUDY

Material Property	Value
Density	8.22 Mg/m <sup>3</sup>
Poisson's Ratio	0.294
Young's Modulus	208 GPa

structure the wedges that are built into, and likely sensitivity to defects by assessing the localization of the ultrasonic energy. The tools are intended to provide the scientific basis for utilizing edge modes in real structures.

Beyond establishing a theoretical appreciation of the capabilities of edge-modes, there is also a standing practical challenge in their excitation and detection. In cases where the wedge has a free end, shear transducers may be used for excitation and detection [20], but in closed-loop wedges such as the seal fin, there is no free end for transduction. In such cases, in order to excite and detect the edge mode, it is necessary to laterally flex the wedge using a "footprint" significantly less than a wavelength; in practice, this requires excitation and detection through a submillimeter diameter footprint. Existing studies rely on excitation by laser [5], [21] or millimeter-scale piezoelectric transducers [22] and detection by laser [5], [21], [23] or electromagnetic acoustic transducers (EMATs) [22]. A piezoelectric-based dry-coupled transducer

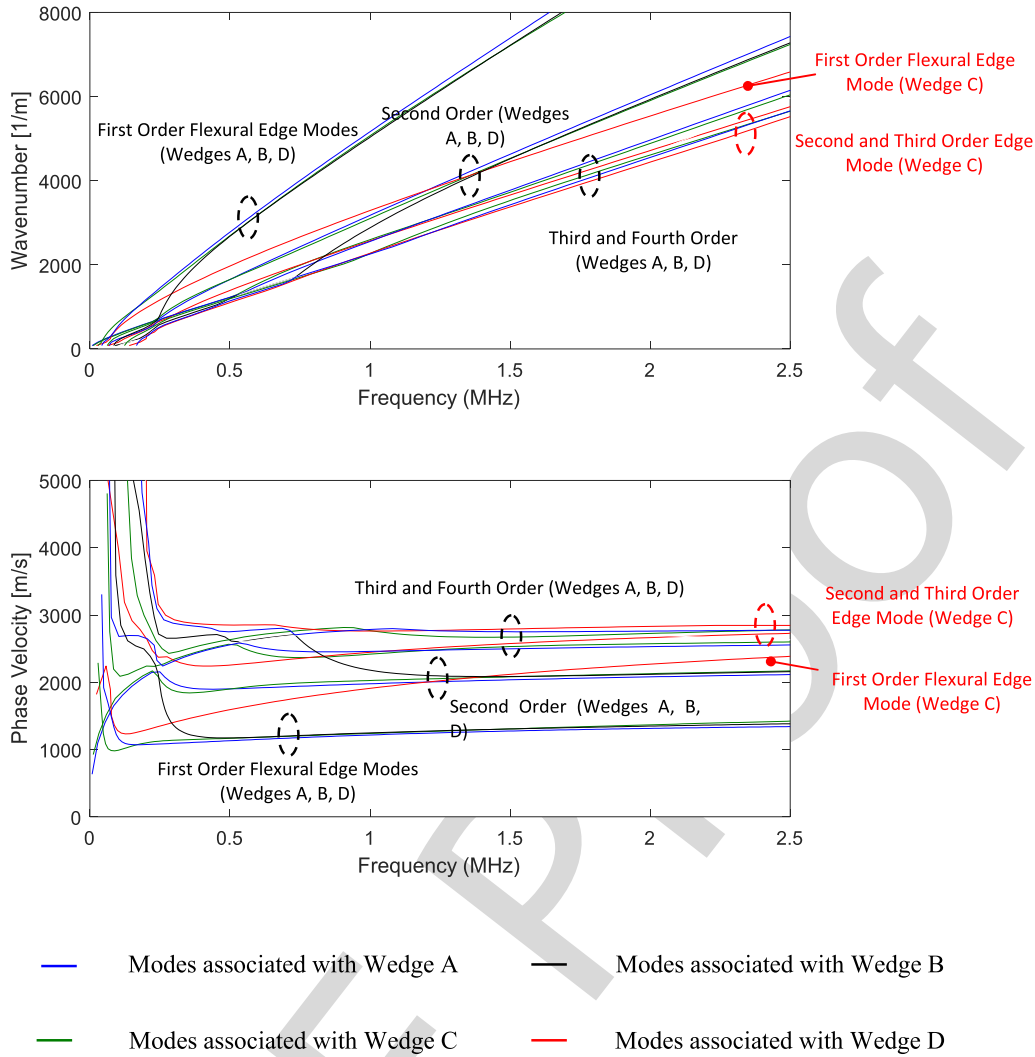


Fig. 4. Dispersion curves of the first 14 edge modes of the body shown in Fig. 3 with material properties shown in Table I. Solutions calculated using an SAFE solver programmed in MATLAB.

124 system has been developed that is capable of pulse-echo  
 125 excitation and detection of edge waves; this development will  
 126 enable use of edge waves in industrial applications.

127 This article starts with a demonstration of the SAFE  
 128 methodology for establishing the dispersion characteristics of  
 129 various arbitrarily shaped wedge-like structures with finite  
 130 geometry. A comparison is made between the edge modes in  
 131 ideal wedges, and wedge with irregular cross section is made  
 132 throughout. A further demonstration is then given to illustrate  
 133 the frequency-dependent localization of ultrasonic energy; this  
 134 is used to evaluate both leakage and sensitivity to tip defects.  
 135 The piezoelectric-based dry-coupled transducer system will  
 136 then be described and demonstrated. This article concludes  
 137 with the experimental demonstration of the inspection method-  
 138 ology on an example jet engine seal fin with simulated defects.

## 139 II. SAFE ANALYSIS OF FEATURE-GUIDED WAVES IN 140 WEDGE-LIKE FEATURES

### 141 A. SAFE Background

142 The SAFE methodology has been outlined in numerous  
 143 previous publications [11], [12], [24]–[26] but will be briefly  
 144 outlined here for completeness. The methodology allows the

145 calculation of the properties of waves in waveguides of  
 146 arbitrarily shaped cross section. The SAFE method requires  
 147 the geometry of the cross section of the waveguide to be  
 148 represented by a 2-D FE discretization and assumes a prismatic  
 149 geometry, so there is no geometric variation along its axis and  
 150 the behavior in the propagation direction can be written in an  
 151 analytical form

$$152 \quad u_j(x, y, z, t) = U_j(x, y)e^{i(kz - \omega t)} \quad (1)$$

153 in which  $k$  is the wavenumber,  $\omega = 2\pi f$  is the angular  
 154 frequency,  $f$  is the frequency,  $t$  is the time variable, and the  
 155 subscript  $j = 1, 2, 3$ .  $i$  is the imaginary number  $(-1)^{1/2}$ . The  
 156 function  $U_j$  represents the behavior in the cross section of  
 157 the waveguide. For general anisotropic media, the equation of  
 158 dynamic equilibrium is written in the following form of an  
 159 eigenvalue problem:

$$160 \quad c_{ijl} \frac{\partial^2 U_j}{\partial x_q \partial x_l} + I(c_{i3jl} + c_{ij3}) \frac{\partial(kU_j)}{\partial x_q} - kc_{i3j3}(kU_j) + \rho\omega^2 \delta_{ij} U_j = 0 \quad (2) \quad 161$$

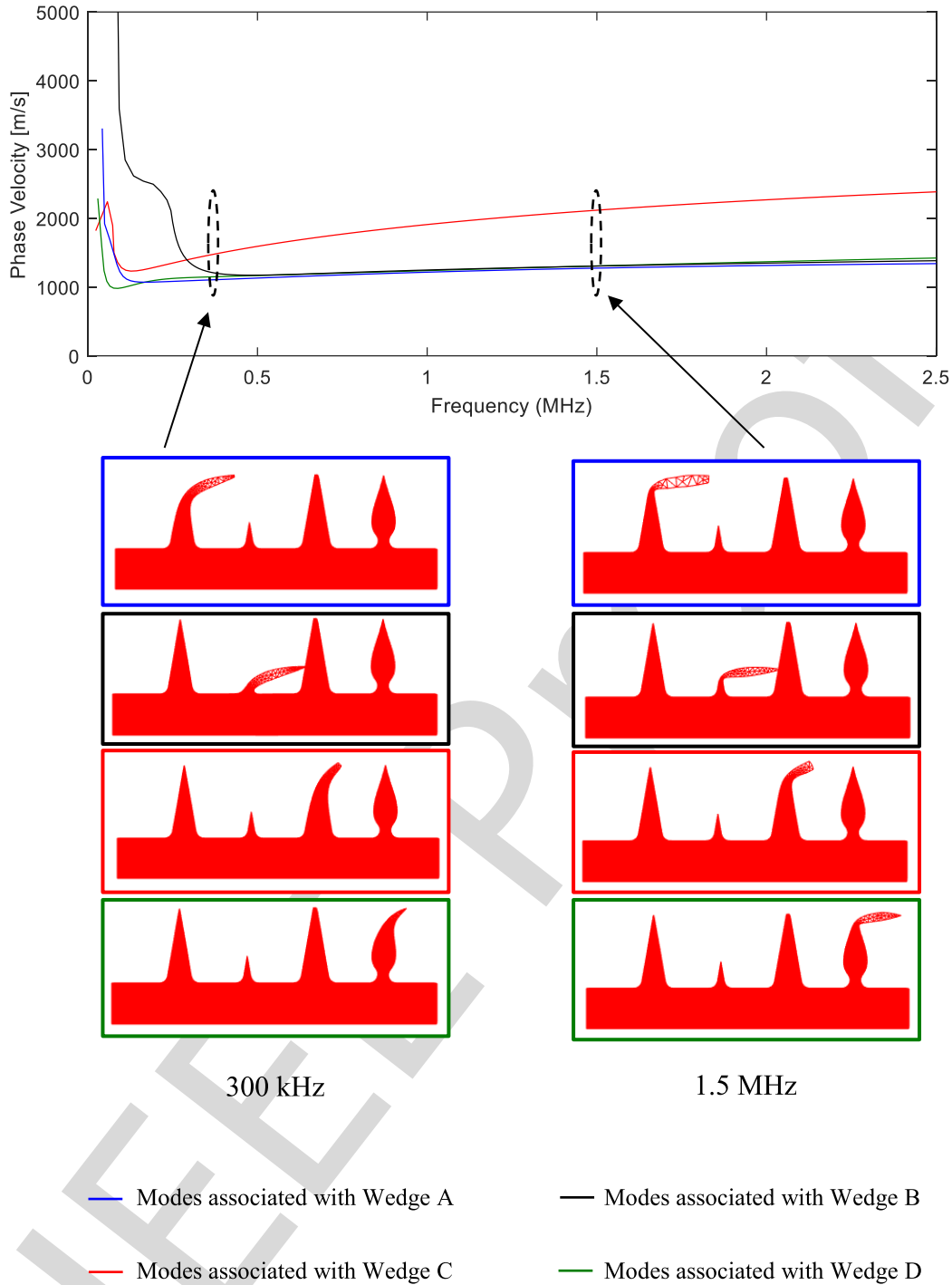


Fig. 5. Dispersion curves of the first-order flexural edge modes for the four-wedge structures shown in Fig. 3 with material properties shown in Table I. Solutions calculated using an SAFE solver programmed in MATLAB. Also shown are the mode shapes (arbitrary displacement) of the 2-D discretization at 300 kHz and 1.5 MHz.

with summation over the indices  $j = 1, 2, 3$  and  $q, l = 1, 2$ . The coefficients  $c_{ijkl}$  are the stiffness moduli,  $\rho$  is the density, and  $\delta_{ij}$  is the Kronecker symbol.

For chosen values of angular frequency  $\omega$ , eigenvalues of complex wavenumber  $k$  are found, in which the real part describes the harmonic wave propagation, while its imaginary part presents the attenuation. Many cases of study address waveguides with zero attenuation, which requires only the solution of real eigenvalues, but the possibility of attenuation must be included in the formulation (using the

complex  $k$  representation) for waveguides where there might be loss of energy by material damping or by leakage into attached or adjacent materials. Each solution at a chosen frequency reveals the wavenumbers of all possible modes at that frequency; then, the full dispersion curve spectrum is constructed by repeating the eigenvalue solutions over the desired range of frequencies.

An in house MATLAB (The Mathworks, Inc., 2014) script was used for the real wavenumber solutions. This is then followed by a separate study using COMSOL

172  
173  
174  
175  
176  
177  
178  
179  
180  
181

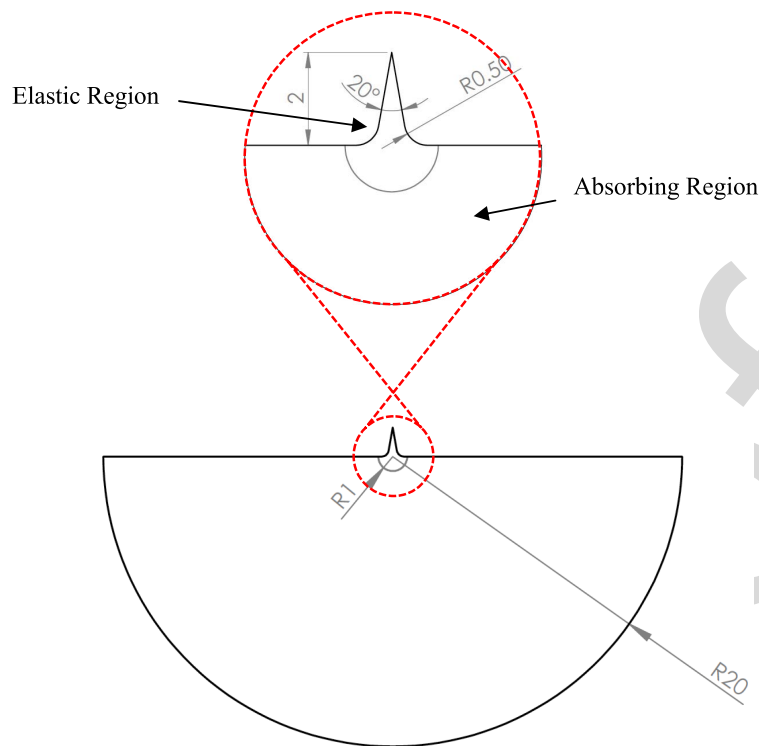


Fig. 6. Illustration of the model of an example wedge feature built into a semicircular body to investigate localization of ultrasonic energy. The wedge is elastic, while the surrounding region is absorbing.

182 (Comsol Inc., 2012), which includes an absorbing boundary  
 183 layer in order to investigate possible attenuation by leak-  
 184 age [27].

### 185 B. SAFE Analysis of Dispersion Characteristics

186 In this study, a hypothetical component with four wedges  
 187 built into it has been devised for demonstrative purposes,  
 188 as shown in Fig. 3. The geometries have been selected to  
 189 illustrate the forms of geometric characteristic that arises in  
 190 waveguides of interest such as the example case of engine  
 191 drum seal fins where multiple wedges share a common base  
 192 structure. The wedges, labeled A–D, all taper with an angle  
 193 of  $20^\circ$  but are each different according to: A) the most ideal  
 194 of the wedges, albeit of finite length and built into a larger  
 195 structure; B) shortened length; C) truncated apex; and D)  
 196 nonstraight sided. The engine drum seal fin of interest in  
 197 this study is similar to Tip C, being of both finite length  
 198 and containing a truncated tip. The dispersion of the edge  
 199 waves is influenced by the solid base, but the detail of it is  
 200 unimportant for the purpose of this study. In principle, there  
 201 may be coupling due to the common base, but it will be shown  
 202 that this is insignificant due to the localized nature of the  
 203 edge modes. Using a common base was chosen for ease of  
 204 computation as all wedges could be evaluated using a single  
 205 model. For this analysis, a MATLAB code was used to find  
 206 the real  $k$  solutions. The solver identified the first 14 modes  
 207 and their dispersion characteristics up to 2.5 MHz. Like the  
 208 seal fins of interest, the hypothetical component is assumed  
 209 to be composed of IN718 material, with properties given

in Table I. The wavenumber and phase velocity are plotted  
 against frequency in Fig. 4. The solver allowed identification  
 of the different modes, as labeled.

The key to understanding the dispersion characteristics  
 of the edge modes is the frequency-dependent localization.  
 Fig. 5 shows only the first-order flexural edge modes for each  
 of the four wedges for improved clarity, together with the  
 corresponding displacement fields. It is shown that the modes  
 become increasingly localized at higher frequency.

The first consequence of the increased localization is that  
 the three nontruncated wedges (A, B, and D) converge to the  
 same high-frequency solutions. At low frequencies, the modes  
 interact with the nonwedge-like structures making the mode  
 dispersive. At higher frequencies, the modes become localized  
 only to the wedge tips (which are identical) and so the  
 dispersion characteristics must converge. This convergence  
 appears at the highest frequency for Wedge B as it requires the  
 greatest localization before it becomes insensitive to the built-  
 in base; the mode shape and dispersion curves shown in Fig. 5  
 indicate its occurrence at around 300 kHz. Equivalent behavior  
 can be observed in the higher order edge modes. Successively  
 higher order modes are less localized, and therefore, higher  
 frequencies are required to constrain the mode to within the  
 wedge tip and for the dispersion curves to converge.

The second consequence of the localization is that the  
 nontruncated wedges converge to be nondispersive. At  
 sufficiently high frequency, the edge modes become wholly  
 localized to the wedge tip and so are insensitive to the  
 remaining structure that causes dispersion. The nontruncated  
 wedge tips may be considered ideal and therefore are

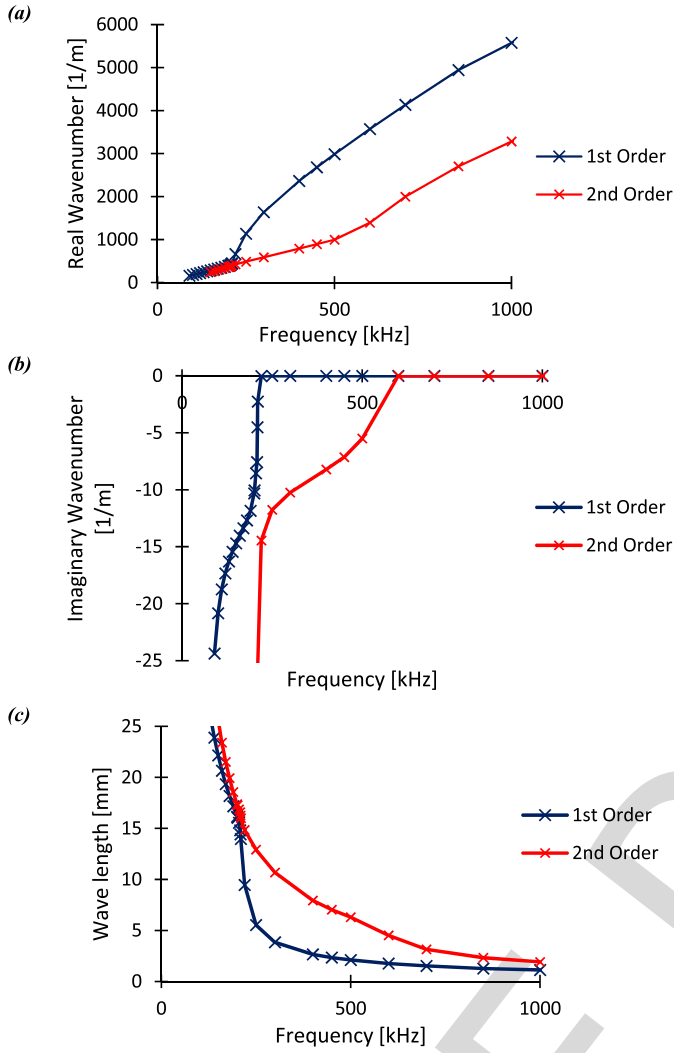


Fig. 7. Results of the SAFE study illustrated in Fig. 6. (a) Real part of wavenumber. (b) Imaginary part of wavenumber. (c) Wavelength.

nondispersive. The high-frequency asymptotic behavior is dictated by the nondimensional wedge angle and the nondispersive phase velocity may be calculated analytically from the analysis presented in [4]. For the material properties in Table I, the shear velocity is 3127 m/s, and for a  $20^\circ$  tip, the phase velocity for the first three wedge modes are 1103, 2159, and 3226 m/s, respectively. This is in good agreement with the high-frequency asymptotic values shown in Fig. 4.

Tip C has a truncated tip, which is of interest due to the impossibility of fabricating a perfectly sharp wedge. The truncation creates a length scale that in turn makes it dispersive. McKenna *et al.* [10] calculated that the dispersion measure that is defined as

$$C \equiv \frac{\omega}{v_g} \frac{dv_g}{d\omega} \quad (3)$$

where  $v_g$  is the group velocity and a function of the truncation width,  $h_0$  (0.3 mm in Wedge C), and the angular frequency  $\omega$  according to

$$C = 6 \left( \frac{2\pi}{\lambda} \frac{h_0}{\tan \frac{\theta}{2}} \right)^2 \quad (4)$$

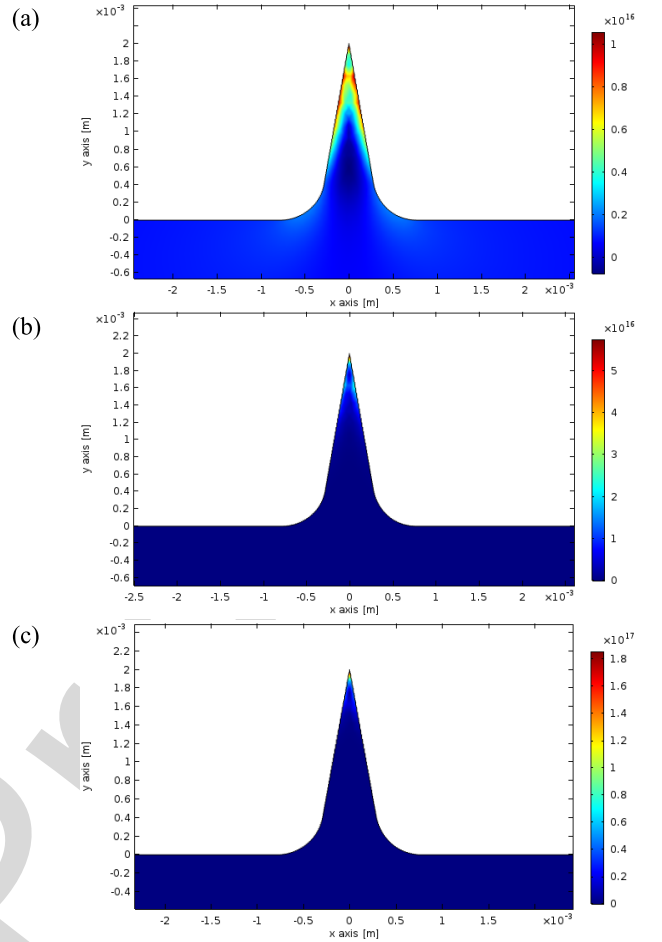


Fig. 8. Power flow density of the first-order flexural edge mode at 200 kHz, 500 kHz, and 1 MHz for the feature shown in Fig. 6. The color indicates the axial power flow (for unit power flow, note different color scales at different frequencies). (a) 200 kHz. (b) 500 kHz. (c) 1 MHz.

where  $\beta = 2\pi/\lambda$ . The dispersion is reduced when the truncation width is small compared with the localization, and this may be achieved by having a small truncation width or reducing the frequency (a longer wavelength).

The seal fins of interest closely resemble Wedge C. The first-order flexural edge wave is dispersive over the full frequency range of interest: at low frequency due to the finite length of the fin and interaction with the base structure and at high frequency due to the increasing significance of the influence of the truncation. Despite this, it is assessed that the dispersion is sufficiently low for practical use above approximately 500 kHz and therefore may be suitable for NDE inspection.

### C. SAFE Analysis of Leakage

Utilizing edge modes for NDE requires that both the transmitted and reflected waves can propagate effectively along the wedge over sufficient distances to provide component coverage from a reasonable number of measurement points. From the previous analysis, it was shown that at high frequencies, the edge modes are localized to the wedge tips, but at lower frequencies, in real components, they may interact with nonwedge features, and this interaction causes energy from

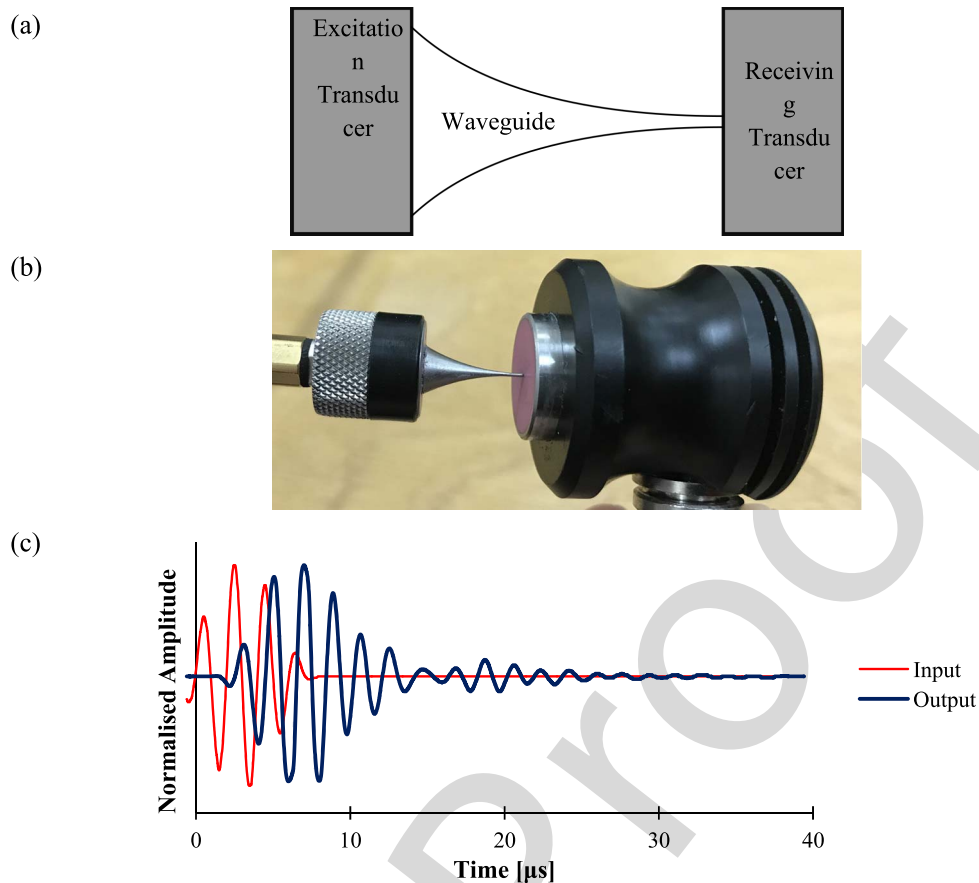


Fig. 9. (a) Illustration of the experimental arrangement. (b) Photograph of the experimental arrangement. (c) Comparison of the excitation and receiving signal through the waveguide.



Fig. 10. Photograph showing inspection of a seal fin feature of a jet engine drum.

279 the guided wave to travel out of the feature of interest into the  
 280 surrounding media, a process known as leakage [24]. The wave  
 281 attenuation due to leakage has to be assessed to ensure that the  
 282 mode excited could propagate along the structure effectively.

283 The phenomenon of wave mode leakage could be quantified  
 284 using SAFE formalism, and in this case, the SAFE analysis  
 285 was implemented using Comsol finite element software. Con-  
 286 sidering the four wedges presented in Section II-B, Wedge  
 287 B is likely to have the greatest leakage as it is the shortest  
 288 and therefore requires greater localization for the energy to

be contained wholly within the wedge; we therefore chose to  
 study this wedge in greater detail.

289  
 290  
 291 The implementation in Comsol software comprised the  
 292 wedge built into a semicircular base, as shown in Fig. 6.  
 293 The wedge and inner portion of the semicircle are modeled as  
 294 perfectly elastic, while the outer portion of the semicircle is  
 295 absorbing modeled by an absorbing material, having the same  
 296 stiffness properties but also damping properties. The damping  
 297 properties are introduced as a growing function with radius,  
 298 following the approach that has been documented in [24].



Any attenuation will, therefore, be a result of wave modes leaking into the absorbing region. The solutions to the wave equation for the modeled cross section will be complex, the real part providing the real wavenumber and the imaginary part indicating the effective attenuation or leakage.

The complex wavenumber and wavelength are shown in Fig. 7 for the first- and second-order edge modes. In both cases, the magnitude of the imaginary part of the wavenumber increases with decreasing frequency, and this is expected as the mode becomes less localized and interacts with the attenuating absorbing region. The second-order mode is less localized, and therefore, leaking will occur up to higher frequencies. The root of the first-order mode becomes entirely real above around 220 kHz, while the root of the second-order mode becomes entirely real above 500 kHz, indicating that the edge mode is entirely localized to the elastic region above these frequencies and effective propagation can be expected.

For inspection purposes, the presence of higher order modes with faster velocities (see Fig. 4) may interfere with the interpretation of inspection results, which utilize the first-order mode. In this regard, leakage-related attenuation of the higher order modes is beneficial. The results of Fig. 7 show that for this particular geometry at 500 kHz, the imaginary part of the first-order mode is zero, while the second-order mode is  $-5.5 \text{ m}^{-1}$ . This indicates that if excited, the second-order mode will be attenuated by 48 dB/m and therefore fall below the noise level within a meter of propagation, i.e., no influence on the detection of flaws is expected from higher order modes. It is worth noting that this particular geometry is only 2 mm high and taller wedges will have less leakage.

Practically, to provide full coverage for the inspection of a circumferential seal fin and to exclude interference from higher order modes, measurements are taken from at least two locations. As the interpretation of any signal is done on the assumption of wave speed of the first-order mode, any noise from an unwanted mode will indicate different locations for each test and so can be ignored.

To conclude this analysis, as the seal fins of the jet engine are longer than the 2 mm in this example, we can conclude that down to at least 220 kHz, the localization of the first-order mode is sufficient that leakage will be negligible, leading to effective propagation. It should, therefore, be possible to screen long lengths of the seal fin structure from a single inspection location by choosing to inspect at frequencies greater than around 200 kHz. Higher order modes will also propagate without leakage-related attenuation at higher frequencies; this provides a motivation to use lower frequencies that must be balanced against the increased dispersion.

#### D. SAFE Analysis of Anticipated Reflection From Defects

Given the very localized nature of the edge modes, it is anticipated that the sensitivity to defects in the wedge tips is very high. This has recently been shown for an ideal wedge using FE simulations and experimentally by Chen *et al.* [5], obtaining reflection coefficients (defined as the reflected

energy divided by incident energy) of  $>0.5$  from 0.3-mm defects in  $40^\circ$  wedges at 2 MHz.

The SAFE analysis described in Section II-A may also be used to approximate the likely response to candidate defects.

Fig. 8 shows the power flow density into the cross section of the fin calculated from the stress and particle velocity obtained by the model. The power flow fields have been normalized to the peak power flow density of the cross section to allow comparison across the different frequencies. This corresponds to the wave energy moving in the propagating direction (perpendicular to the cross section) per unit time and area. The presence of a defect at the wedge will disrupt the power flow; the reflection from a defect will increase with its size and the transmission will decrease.

As anticipated, it can be seen that the power flow becomes more localized to the fin tip as frequency increases. The reflection coefficient of a through crack will be roughly proportional to the fraction of the power flow that it interrupts; assuming that the defect is situated at the wedge tip, then the reflection coefficient will increase with frequency and defect length (measured from the tip of the wedge to the base).

Fig. 8 shows that a defect of just 0.25 mm would interrupt the vast majority of energy of the first-order flexural edge mode at 500 kHz, indicating that the reflection coefficient is expected to be very high. Further quantitative analysis on reflection and transmission coefficients is possible, as shown by Chen *et al.* [5], and SAFE analysis may complement this effort.

The inspection requirement for the seal fin inspection problem is to detect a 0.75-mm radial tip defect. The analysis presented here indicates that when using frequencies of the order of 100 kHz and above, the reflection coefficient is likely to be very high, making the first-order flexural edge mode well suited to the inspection problem. It should be noted that there may potentially be a negative side of the high sensitivity to tip defects; if the mode is highly localized to the tip, then transmission may be impeded by scattering from roughness along the length of the wedge tip. It may, therefore, be necessary to find a compromise between sensitivity and sought defects while suppressing the effects of benign tip roughness.

### III. EXCITATION AND DETECTION

In order to excite the edge waves, the transducer must laterally displace the wedge tip, as shown in Fig. 2. It must do so with a transducer footprint diameter of less than half a wavelength, as material more than half a wavelength away should be free to be displaced in the opposite direction. Furthermore, practical studies by Fromme *et al.* [28] have indicated that smaller is better; in practice, we use a “rule-of-thumb” of one-fifth, but interested readers could follow up on the work of Fromme or the earlier work by Wilcox cited therein. Fig. 7 shows the calculated wavelengths of the edge mode for the example wedge feature used in Sections II-A and II-B. It can be seen that the transducer footprints of submillimeter are required.

A piezoelectric-driven pointed waveguide is proposed, which will focus on the energy to a small, point-like,

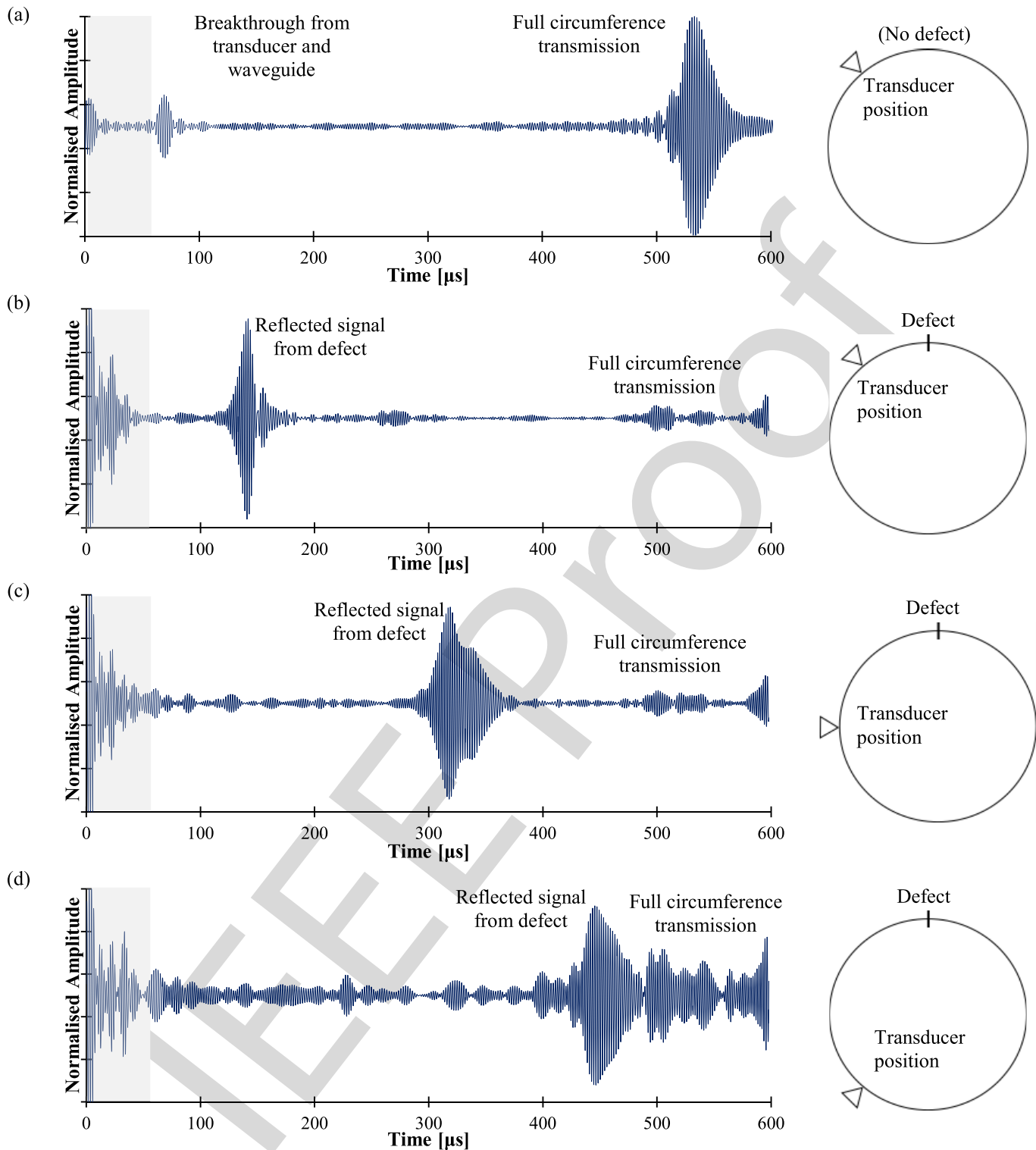


Fig. 11. A-Scan from (a) defect-free seal fin and (b)–(d) seal fin with a 0.75-mm radial defect. 500 kHz, five-cycle toneburst; 30-V output; 600- $\mu$ s sample length; 50-dB receiver gain; 400–600-kHz receiver bandpass filter; 16 averages. Amplitude of each signal is individually normalized to the maximum of the signal beyond 100  $\mu$ s.

412 footprint, as shown in Fig. 9(a) and (b). The power trans- 418  
 413 fer efficiency through the waveguide is not critical as 419  
 414 the input power can simply be increased to achieve the 420  
 415 desired output. Instead, the key performance parameter is the 421  
 416 fidelity, and the signal transmitted through the tip should 422  
 417 not be too prolonged or distorted by reverberations or

undesired modes in the waveguide as a prolonged signal 418  
 will act to mask any reflected signals being received. The 419  
 design of waveguides to suppress the undesired modes is 420  
 an active field of research; the design of the waveguide 421  
 used in this study was inspired by the flexural damping 422  
 design of [29]. 423

It was found that the capability of the transducer system was not particularly sensitive to the details of the design, but for completeness, the design used in this study was as follows. The transducer is a commercially available Olympus, 10-mm diameter, 2.25-MHz center frequency, piezoelectric transducer (part number: U8477174). The waveguide is 6 mm diameter at the base, <0.5 mm diameter at the tip, and 11 mm long. It is fabricated from 316 stainless steel and the curvature is approximately cubic. The excitation pulse is not dispersion compensated.

A simple experiment is conducted to demonstrate the waveguide performance; two transducers are used in a simple through transmission arrangement, as shown in Fig. 9(a) and (b). Measurements were taken with a standard flaw detector within its normal range of operation. The excitation and received signals are shown in Fig. 9(c). Only a slight reverberation is evident following the initial wave that is unlikely to be an issue in most applications. The reverberations may be further suppressed if necessary by more advanced waveguide design or damping of the free surfaces.

#### IV. EXPERIMENTAL DEMONSTRATION

An example jet engine drum is used to demonstrate the use of edge waves for screening of defects, as shown in Figs. 1 and 10. The drum has several seal fin features, including two with diameters of approximately 420 mm. The wedge feature was similar to Wedge C from Fig. 3, with a 0.3-mm-wide flat truncation. The heights of the wedges were greater than the wedge used for the leakage analysis, and therefore, minimal leakage is anticipated. The two fins were otherwise identical except one that was defect free, while in the other, a 0.75-mm radial EDM notch was introduced to replicate a defect.

The piezoelectric transducer with pointed tip waveguide, as shown in Fig. 9, was used for the inspections in the pulse-echo configuration. The transducer system was lightly pressed normal to the wedge, causing a lateral flexural excitation, relying on dry coupling. A standard handheld ultrasonic flaw detector was used with a 30-V output, 500-kHz five-cycle toneburst output. The receiver chain had 50-dB amplification and a 400–600-kHz bandpass filter, ~100 averages were taken.

Fig. 11(a) shows an A-scan taken of the defect-free component. The first ~50  $\mu$ s show the transmitted signal and reverberations as the ultrasound passes through the waveguide into the component. At around 510  $\mu$ s, a wave packet arrives that has traveled around the full circumference of the component, a distance of approximately 1.32 m. This result shows the effectiveness of the transducer system and also the excellent propagation of the edge mode.

The noise observed in this experiment is coherent. It is believed to originate from excitation of undesired modes, interaction with the bulk of the body, and imperfect surface condition. Two or more readings from separate locations will help suppress the influence of coherent noise.

Fig. 11(b)–(d) shows the A-scans of the defective component, while the transducer location is moved successively further away from the defect. In each case, the reflection

from the defect is very apparent, rising well above the noise floor. A typical signal-to-noise ratio (SNR) of 28 dB was calculated from the maximum amplitude between 100–200  $\mu$ s (the signal) and 200–400  $\mu$ s (the noise) from Fig. 11(b).

It is, of course, apparent that at least two inspection locations are required for a full coverage of a circular component. “Blind spots” are created in the near field of the transducer due to breakthrough and also diametrically opposite from the transducer due to the signal transmitted around the full circumference arriving at the same time as a defect reflection. Minimizing the edge mode dispersion and improving the waveguide fidelity are the key to minimizing the extent of the blind spots. It should be emphasized that efforts have not been made to size the defects but only to screen for their presence. It is envisaged that after they have been identified, they may be sized with a more local inspection procedure.

#### V. CONCLUSION

This article provides the scientific basis to develop practical NDE tools for the inspection of wedge features, demonstrating the analytical tools required for characterization of edge modes in arbitrarily shaped wedge-like structures together with the practical tools required for inspection in industry.

Introducing irregular features to a wedge-like geometry provides length scales, which may cause the edge wave propagating along them to become dispersive. SAFE analysis provides an opportunity to establish the dispersion characteristics of arbitrarily shaped wedge-like features to assess their suitability for guided wave inspection. The SAFE analysis shows that increasing the ultrasonic frequency leads to increasing localization of the edge modes to the wedge tips. If the tip of the wedge approximates an ideal wedge (straight edged and is not truncated), then at sufficiently high frequencies, the energy becomes sufficiently focused to the dimensionless tip that it becomes nondispersive.

For wedges with truncated tips, which will be true of any real fabricated wedge to some extent, the dispersion measure is proportional to the squared ratio of the truncation width and the wavelength. The truncation provides a length scale that will be increasingly significant at higher frequencies; for a given wedge geometry, the dispersion can be suppressed by reducing the frequency (increasing the wavelength). In such cases, the edge mode will be dispersive over the full frequency range of interest: at low frequency due to the finite length of the fin and at high frequency due to the increasing significance of the truncation. An understanding of the science presented in this article is therefore crucial; the frequency must be chosen cognizant of the opposing requirements for sufficient localization to avoid interaction with the base structure, but not too localized for the influence of the truncation to become too significant.

SAFE analysis allows the assessment of the anticipated effect of attenuation causing leakage into surrounding structures. It was shown using one example geometry that by increasing the measurement frequency, the ultrasonic energy could be sufficiently localized into the tip so that it becomes insensitive to the surrounding structure allowing good propagation. SAFE analysis also offers a tool for the assessment of

likely sensitivity to defects by analyzing the power flow in the feature. The more energy that a defect interrupts, the greater the likely reflection coefficient; this could be manipulated by focusing the energy by choice of measurement frequency.

The practical use of the short-wavelength edge waves for NDE purposes requires transducers with a submillimeter point-like footprint. A simple piezoelectric transducer system with a pointed tip waveguide has been presented for this purpose. The transducer system may be dry coupled and used in a pitch-catch configuration.

For the example application of the seal fin in this article, 500 kHz was found to be suitable; balancing the needs of limiting dispersion, sensitivity, and wavelength limited transducer footprint. The seal fins of an ex-service engine drum have been used to demonstrate the use of edge modes for defect screening. The demonstration shows the propagation of the edge modes over distances of greater than 1 m and the clear identification of defects from the reflected signals; a typical SNR of 28 dB was achieved.

#### ACKNOWLEDGMENT

The authors would like to thank D. Fan and X. Yu of Nanyang Technological University for support with the semi-analytical finite-element (SAFE) analysis of Section II-C and Guided Ultrasonics Ltd. for developing the MATLAB-based SAFE code used in Section II-B.

#### REFERENCES

- [1] P. Lagasse, "Analysis of a dispersion free guide for elastic waves," *Electron. Lett.*, vol. 8, pp. 372–373, 1972.
- [2] S. L. Moss, A. A. Maradudin, and S. L. Cunningham, "Vibrational edge modes for wedges with arbitrary interior angles," *Phys. Rev. B, Condens. Matter*, vol. 8, no. 6, pp. 2999–3008, Sep. 1973.
- [3] V. V. Krylov, "Geometrical-acoustics approach to the description of localized vibrational modes of an elastic solid wedge," vol. 35, no. 1, pp. 137–149, 1990.
- [4] A. P. Mayer, B. W. Fakultät, V. V. Krylov, and A. M. Lomonosov, "Guided acoustic waves propagating at surfaces, interfaces and edges," in *Proc. IEEE Int. Ultrason. Symp.*, Oct. 2011, pp. 2046–2052.
- [5] M. Chen, S. Tesng, P. Lo, and C. Yang, "Characterization of wedge waves propagating along wedge tips with defects," *Ultrasonics*, vol. 82, pp. 289–297, 2018.
- [6] V. V. Krylov, "A new type of vibration damper based on flexural wave propagation in laminated wedges of power-law profile," *J. Acoust. Soc. Amer.*, vol. 110, no. 5, p. 2654, 2001.
- [7] V. V. Krylov and F. J. B. S. Tilman, "Acoustic 'black holes' for flexural waves as effective vibration dampers," *J. Sound Vib.*, vol. 274, nos. 3–5, pp. 605–619, 2004.
- [8] M. de Billy, "On the scattering of antisymmetric edge modes," *J. Acoust. Soc. Amer.*, vol. 101, no. 6, pp. 3261–3269, 1997.
- [9] V. V. Krylov, "Wedge elastic waves, with applications to ultrasonic non-destructive testing," in *Proc. 55th Annu. Brit. Conf. Non-Destruct. Test.*, 2016.
- [10] J. Mckenna, G. D. Boyd, and R. N. Thurston, "Plate theory solution for guided flexural acoustic waves along the tip of a wedge," *IEEE Trans. Sonics Ultrason.*, vol. SU-21, no. 3, pp. 178–186, Jul. 1974.
- [11] L. Gavrić, "Computation of propagative waves in free rail using a finite element technique," *J. Sound Vib.*, vol. 185, no. 3, pp. 531–543, 1995.
- [12] T. Hayashi, W.-J. Song, and J. L. Rose, "Guided wave dispersion curves for a bar with an arbitrary cross-section, a rod and rail example," *Ultrasonics*, vol. 41, pp. 175–183, May 2003.
- [13] P. Wilcox, M. Evans, O. Diligent, M. Lowe, and P. Cawley, "Dispersion and excitability of guided acoustic waves in isotropic beams with arbitrary cross section," *Rev. Quant. Nondestruct. Eval.*, vol. 21, pp. 203–210, 2002.

- [14] Z. Fan and M. J. S. Lowe, "Elastic waves guided by a welded joint in a plate," *Proc. Roy. Soc. A, Math., Phys. Eng. Sci.*, vol. 465, no. 2107, pp. 2053–2068, 2009.
- [15] Z. Fan, M. Castaings, M. J. S. Lowe, C. Biateau, and P. Fromme, "Feature-guided waves for monitoring adhesive shear modulus in bonded stiffeners," *NDT&E Int.*, vol. 54, pp. 96–102, 2013.
- [16] X. Yu, Z. Fan, M. Castaings, and C. Biateau, "Feature guided wave inspection of bond line defects between a stiffener and a composite plate," *NDT&E Int.*, vol. 89, pp. 44–55, Jul. 2017.
- [17] T. Yu, K. Yoshida, and H. Shi, "A 2-D mesoscopic model for the evaluation of creep damage induced by void growth in polycrystalline metals," *Acta Metallurgica Sinica, English Lett.*, vol. 24, no. 3, pp. 213–219, 2011.
- [18] X. Yu, M. Ratssepp, and Z. Fan, "Damage detection in quasi-isotropic composite bends using ultrasonic feature guided waves," *Compos. Sci. Technol.*, vol. 141, pp. 120–129, Mar. 2017.
- [19] X. Yu, P. Zuo, J. Xiao, and Z. Fan, "Detection of damage in welded joints using high order feature guided ultrasonic waves," *Mech. Syst. Signal Process.*, vol. 126, pp. 176–192, Jul. 2019.
- [20] M. De Billy, "Acoustic technique applied to the measurement of the free edge wave velocity," *Ultrasonics*, vol. 34, no. 6, pp. 611–619, 1996.
- [21] J. Jia, L. Wang, Z. Shen, L. Yuan, and X. Ni, "Study of mode transformation and energy attenuation of wedge waves with different apex angles by laser ultrasonic techniques," *Sci. China Phys., Mech. Astron.*, vol. 55, no. 4, pp. 593–598, Apr. 2012.
- [22] J. R. Chamuel, "Edge waves along immersed elastic elliptical wedge with range dependent apex angle," in *Proc. IEEE Ultrason. Symp.*, Oct./Nov. 1993, pp. 313–318.
- [23] P. Hess, A. M. Lomonosov, and A. P. Mayer, "Laser-based linear and nonlinear guided elastic waves at surfaces (2D) and wedges (1D)," *Ultrasonics*, vol. 54, no. 1, pp. 39–55, Jan. 2014.
- [24] M. Castaings and M. Lowe, "Finite element model for waves guided along solid systems of arbitrary section coupled to infinite solid media," *J. Acoust. Soc. Amer.*, vol. 123, no. 2, pp. 696–708, 2008.
- [25] L. Gavrić, "Finite element computation of dispersion properties of thin-walled waveguides," *J. Sound Vib.*, vol. 173, no. 1, pp. 113–124, 1994.
- [26] P. Zuo, X. Yu, and Z. Fan, "Numerical modeling of embedded solid waveguides using SAFE-PML approach using a commercially available finite element package," *NDT&E Int.*, vol. 90, pp. 11–23, 2017.
- [27] D. Fan and X. Yu, "Private communication with Prof. Zheng Fan and Dr. Xudong Yu on COMSOL SAFE Analysis," 2016.
- [28] P. Fromme, P. D. Wilcox, M. J. S. Lowe, and P. Cawley, "On the development and testing of a guided ultrasonic wave array for structural integrity monitoring," *IEEE Trans. Ultrason., Ferroelectr., Freq. Control*, vol. 53, no. 4, pp. 777–785, Apr. 2006.
- [29] V. Kralovic and V. V. Krylov, "Damping of flexural vibrations in tapered rods of power-law profile: Experimental studies," *Proc. Inst. Acoust.*, vol. 29, no. 5, pp. 66–73, 2007.



**Joseph Corcoran** received the M.Eng. and Ph.D. degrees from Mechanical Engineering Department, Imperial College London, London, U.K., in 2011 and 2016, respectively.

He was subsequently appointed as a Research Fellow. He specializes in developing structural health monitoring systems and the use of monitoring data for improved structural integrity diagnostics and prognostics.



**Eli Leinov** received the B.Sc., M.Sc., and Ph.D. degrees in mechanical engineering from Ben-Gurion University, Israel. His Ph.D. research was in the field of hydrodynamic instabilities.

He worked as a Postdoctoral Research Associate with Smart Wells Group, Department of Earth Science and Engineering, Imperial College London, U.K., from 2009 to 2011, with a focus on spontaneous electrical potentials in subsurface geophysical monitoring. He worked as a Postdoctoral Research Associate at the NDE

Group, Department of Mechanical Engineering, Imperial College London, from 2012 to 2017, with a focus on guided wave testing of buried and embedded pipes, and other advanced guided wave applications. In 2018, he joined Guided Ultrasonics Ltd., Brentford, U.K., as a Senior Development Engineer and the Training Division Manager.

AQ:8 673 **Alejandro Jeketo** received the M.Eng. degree in aeronautical engi-  
674 neering and the Eng.D. degree in mechanical engineering from Imperial  
675 College London, London, U.K.  
676 He pursued an interest in aftermarket services following his doctoral  
677 training and currently leads inspection technology development for Civil  
678 Aerospace Repair and Services at Rolls-Royce plc, Derby, U.K.



**Michael J. S. Lowe** received the B.Sc. degree  
679 in civil engineering from The University of Edin- AQ:9  
680 burgh, Edinburgh, U.K., and the M.Sc. and Ph.D.  
681 degrees in mechanical engineering from Imperial  
682 College London, London, U.K.  
683

684 He worked in engineering consultancy from  
685 1979 to 1989, specializing in the application and  
686 development of numerical methods for the solu-  
687 tion of problems in solid mechanics. His principal  
688 clients were in the nuclear power and offshore  
689 oil industries. Since 1989, he has been with the  
690 Department of Mechanical Engineering, Imperial College London, where  
691 he is currently a Professor of mechanical engineering. He has authored  
692 over 250 journal and conference articles relating to ultrasound, guided  
693 waves, numerical modeling, and nondestructive evaluation (NDE). His  
694 current research interests include the use of ultrasound for NDE, with  
695 special interests in guided waves, the interaction of waves with defects  
696 and structural features, and numerical modeling.

697 Prof. Lowe was an elected fellow of the Royal Academy of Engineering,  
698 London, for his research contributions to NDE in 2014.

IEEE PROCEEDINGS